Central Power Research Institute

Vol. 14(1)/105-113, June 2018
ISSN (Print) : 0973-0338
DOI : 10.33686/pwj.v14i1.142192

Power Research

Performance Evaluation of VSC-HVDC Link for Varying AC System Strengths

J. Sreedevi[1*], V. Anuradha[2], Premila Manohar[2] and R. S. Shivakumara Aradhya[3]

[1]Power Systems Division, Central Power Research Institute, Bengaluru – 560080, Karnataka, India; sreedevi@cpri.in

[2]Department of Electrical and Electrinics Engineering, Ramaiah Institute of Technology, Bengaluru – 560054, Karnataka, India

[3]Department of Electrical and Electronics Engineering, Acharya Institute of Technology, Bengaluru – 560107, Karnataka, India

Abstract

Strength of the AC system is one of the important parameters that govern performance of HVDC systems. Even though VSC-HVDC is known to have fewer problems compared to LCC-HVDC at lower system strengths, it is still the topic of research. This paper presents a detailed analysis on the modelling and tuning of the control system of a VSC-HVDC system for varied AC system strengths. Emphasis has been on the tuning of control system parameters considering the effect of AC system strength to improve the transient response of the VSC-HVDC system. A combination of control schemes consisting of DC voltage and AC voltage control at the rectifier and inverter end have been considered. The control parameters are tuned with symmetrical and modulus optimum criteria and found that tuning method is working for weak systems. The VSC-HVDC system is modelled in RSCAD software of RTDS.

Keywords: AC Voltage Control, Active and Reactive Power Control, DC Voltage Control, Proportional Integral (PI), Short Circuit Ratio (SCR) Words, Source Impedance, VSC - HVDC

1. Introduction

Voltage Source Converter (VSC) based High Voltage Direct Current (HVDC) transmission is getting significant attention in recent years. Self-commutated converters have many advantages over the conventional Line Commutated Converters (LCC). VSC-HVDC projects are under implementation despite its high capital investment due to its commutation-free operation and non-requirement of reactive power[1]. LCC-HVDC systems have the history of failing in operation when connected to weak AC grids where the Short Circuit Ratio (SCR) varies from 2 to 3[2]. But VSC is proven to operate even under such conditions, though there are few problems in its performance[3].

There are different control schemes for the VSC-HVDC system and the authors of[4] have studied and compared them. VSC-HVDC is known to have independent control[5] of real and reactive powers with the vector current control[6], which is widely used among several other control techniques and has been under study from the 90s[7,8]. Controller design is based on D-Q model of VSC with parametric optimization[9]. Steady state model of VSC based HVDC system has been developed by feedback compensation and feedforward blocks are also adopted for fast response[10,11]. Transient mathemati- cal model for the VSC based HVDC system supplying passive network in d-q synchronous reference frame is developed and its controllers are designed[12]. The control contains the decoupling

*Author for correspondence

of the current control strategy and having utilized the AC active current to compensate the DC voltage[13].

Among the different combinations of control strategies, studies have been done to verify the best combinations[14,15]and also improve the stability during dynamic performance for multi-infeed applications[16] and industrial applications[17]. VSC-HVDC has been widely utilized for dual infeed HVDC systems, focussing on the effects when connected to lower SCRs[18] or any dynamic loads such as inductive[19] or passive loads[20]. Multi infeed HVDC system consisting of LCC as rectifier and VSC as inverter is simulated[21] and such links are individually studied for comparing its performance with the VSC link[22]. VSC control system is usually based on the use of conventional PI controllers. As there are no such mathematical derivations for obtaining the gains of the PI controller, authors in[23] have developed tuning techniques which enable the system to attain stability during transient conditions. The recent research on improving the stability and robustness of the VSC-HVDC system[24]have been extended to when it is being connected to weak grids[3] and taking into consideration the system impedance or the SCR for calculating the appropriate Phase locked loop gains which have much effect on the system than the PI gains[25–28]. The authors of[29] have carefully analysed the pros and cons of the VSC-HVDC links when connected to weak grids and suggested few solutions for overcoming the issues.

The controls in a VSC-HVDC system play a major role in the operation during transient conditions by controlling the DC voltage and currents. The present work aims to design the controller parameters of VSC-HVDC system taking into effect the effect of AC system strength. Comparison of the time response and damping of the system for different contingencies is analyzed for varying AC system strengths. The control parameters are tuned with modulus optimum and symmetrical optimum[23] tuning techniques for AC systems of different SCRs.

In Section 2, the basic equations are deduced for the design of the control system which is simulated in RSCAD software. Tuning techniques are explained in Section 3. Section 4 presents the simulation of VSC-HVDC system followed by the conclusions.

2. Mathematical Modelling for the Control Of VSC-HVDC

The single line diagram of VSC-HVDC system and its controls is as shown in Figure 1. It consists of AC The venin's equivalent, converter transformer, series filter, voltage source converter and DC line. The nomenclature of various parameters in the diagram is as shown in Table 1.

Table 1. Nomenclature of various parameters

Parameter	Rectifier	Inverter
Internal voltage of the source	E_{SR}	E_{SI}
Voltage at Point of Common Coupling	V_{SR}	V_{SI}
Converter Voltage	V_{CR}	V_{CI}
Source Resistance	R_{SR}	R_{SI}
Source Inductance	L_{SR}	L_{SI}
Transformer Leakage Resistance	R_{TR}	R_{TI}
Transformer Leakage Inductance	L_{TR}	L_{TI}
Filter Inductance	L_{FR}	L_{FI}
DC Capacitance	C_{DCR}	C_{DCI}
DC Line Resistance	R_{LN}	
DC Line Reactance	L_{LN}	

In a VSC-HVDC system, there are four control modes viz: V_{dc} control, P_{dc} control, V_{ac} control and Q_{ac} control in outer control loop depending upon the application. The outer power control loop is used to generate the current references for regulating the output active power and reactive power of the VSC-HVDC link. The typical block diagram of outer control loop is as shown Figure 1. The inner current control loop is implemented in the DQ-frame, based on the equations deduced below from electrical network in Figure 1.

At the inverter side,

$$E_{SI(abc)} - V_{CI(abc)} = R_{SI} i_{abc} + L_{SI} di_{abc}/dt + L_{TI} di_{abc}/dt + L_{FI} di_{abc}/dt \quad (1)$$

Converting the three-phase to two-phase rotating domain with Clarke's transformation

$$E_{SI(\alpha\beta)} - V_{CI(\alpha\beta)} = R_{SI} i_{\alpha\beta} + L_{SI} di_{\alpha\beta}/dt + L_{TI} di_{\alpha\beta}/dt + L_{FI} di_{\alpha\beta}/dt \quad (2)$$

Converting two-phase rotating domain to stationary domain using Park's transformation and $\theta = \omega t$,

$$\begin{aligned} E_{SI(\alpha\beta)} &= E_{SI(dq)} e^{j\omega t} \\ V_{CI(\alpha\beta)} &= V_{CI(dq)} e^{j\omega t} \\ i_{(\alpha\beta)} &= i_{(dq)} e^{j\omega t} \end{aligned} \quad (3)$$

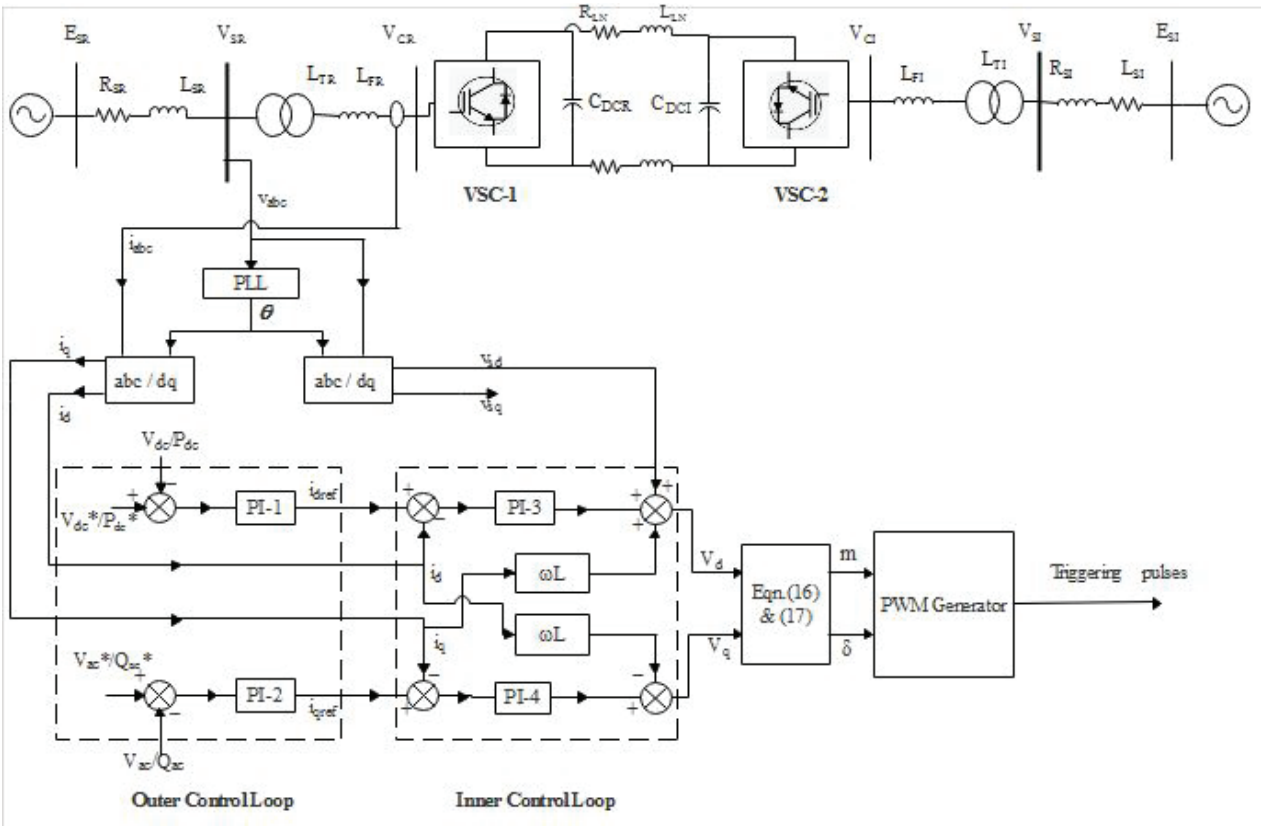

Figure 1. VSC-HVDC system and its controls.

From the above, the dq-equations in the matrix form are given as:

$$\begin{bmatrix} E_{SId} \\ E_{SIq} \end{bmatrix} - \begin{bmatrix} V_{CId} \\ V_{CIq} \end{bmatrix} = R \begin{bmatrix} i_d \\ i_q \end{bmatrix} + \omega L \begin{bmatrix} 0 & 1 \\ -1 & 0 \end{bmatrix} \begin{bmatrix} i_d \\ i_q \end{bmatrix} + L \frac{d}{dt} \begin{bmatrix} i_d \\ i_q \end{bmatrix} \quad (4)$$

here $L = L_{SI} + L_{TI} + L_{FI}$

Because, the commutating transformer is Y/Δ, the zero sequence component is absent due to Δ connection. The instantaneous power for a three-phase system is

$P = va.ia + vb.ib + vc.ic$

this in terms of dq-frame is

$[P_{abc}] = [K][P_{dq0}]$

where

$$[K] = \frac{2}{3} \begin{bmatrix} \cos\theta & \cos(\theta-120) & \cos(\theta+120) \\ \sin\theta & \sin(\theta-120) & \sin(\theta+120) \\ \frac{1}{2} & \frac{1}{2} & \frac{1}{2} \end{bmatrix}$$

$$P_{(dq)} = \frac{3}{2} (E_{SI(d)} i_d + E_{SI(q)} i_q) \quad (5)$$

$$Q_{(dq)} = \frac{3}{2} (E_{SI(q)} i_d - E_{SI(d)} i_q) \quad (6)$$

If the *dq* reference frame is selected in such a way that the d-axis is aligned to the phase-A voltage of '*Vs*'. This results in

$$E_{SI(d)} = E_{SI(d)} \quad (7)$$

$$E_{SI(q)} = 0$$

With this alignment, the active power in Equation (5) can be controlled using active current i_d and reactive power can be controlled using the reactive current i_q. The Equations (5) and (6) can be simplified as follows:

$$P = \frac{3}{2} (E_{SI(d)} i_d) \quad (8)$$

$$Q = -\frac{3}{2} (E_{SI(d)} i_q) \quad (9)$$

The Equation (4) can be further modified

$$V_{CI(d)} = (i_{dref} - i_d)^*(K_p + K_i/s) - \omega L i_q + E_{SI(d)} \quad (10)$$

$$V_{CI(q)} = (i_{qref} - i_q)^*(K_p + K_i/s) + \omega L i_d \quad (11)$$

In a sinusoidal PWM, the fundamental-frequency component (V_{CI}) varies sinusoidally and is in phase with the control signal (V_{dc}) as a function of time[13], which gives:

$$V_{CI} = m*Vdc/2 \quad (12)$$

The voltage components of the fundamental control signal in dq-frame are thus deduced as

$$\begin{bmatrix} V_{cd} \\ V_{cq} \end{bmatrix} = \frac{mV_{dc}}{2} \begin{bmatrix} \sin\delta \\ \cos\delta \end{bmatrix} \quad (13)$$

Hence the modulation index for the PWM can be expressed as

$$m = 2\sqrt{(V_{cd}^2+V_{cq}^2)}/V_{dc} \quad (14)$$

$$\delta = \arctan(V_{cd}/V_{cq}) \quad (15)$$

Thus in the controls implemented, δ and m are utilized for the regulation of the active and reactive powers respectively. The dq0 transformation of system equations is advantageous because it allows the use of linear control algorithms and it is easier to design a PID controller for dq0 model which is not possible with the regular three-phase model. These equations are used to implement the controls in RSCAD software of RTDS.

3. Tuning of PI Regulators

3.1 Tuning of Outer Controllers

DC Voltage control loop is tuned by 'Symmetrical Optimum' design criterion which results in a controller that forces the frequency response of the system as close as possible for low frequencies. Using this method, the phase margin is maximized for given frequency. Thereby system can tolerate more delays. The method has well established tuning rules and has good disturbance rejection. Accordingly this design criterion is chosen for tuning of outer DC voltage controller parameters. The PI controls are of the form (K_p+K_i/s). The control parameters K_p and T_i from[23] are

$$K_p = T_c/ a * K *T_{eq} \text{ and } T_i = a^2 *T_{eq}$$

Where a = 3 is the symmetric distance at coros over frequency when roots are real and equal,

$K=V_{dpu}/V_{dcpu}$ = 1 at steady state,

$T_{eq}=1/f_{sw}$ where f_{sw} is switching frequeny and

$Tc=1/ \omega_b *C_{pu}$

The control parameters K_{PI-1} and T_{PI-1} for the V_{dc} outer control from above substitutions become,

$$K_{PI-1}=f_{sw}/(\omega_b *C_{pu}*a) \quad (16)$$

$$T_{PI-1} = 9/f_{sw} \quad (17)$$

where ω_b - Base frequency, C_{pu} - DC capacitance in pu
The control parameters K_{PI-2} and T_{PI-2} for the V_{ac} outer control PI-2 are tuned based on the response of the system. From the Equations (16) and (17) it is evident that tuning of the outer control parameters is independent of AC system strength.

3.2 Tuning of Inner Current Control

In a cascade control structure, the inner loop response must be faster when compared to the speed of response of the outer loop. So, the inner loop is tuned according to 'Modulus optimum' condition because of its fast response and simplicity[23].

The control parameters for modulus optimum are

$$K_p = \tau_{pu} *R_{pu}/2*T_{a,} \text{ and } T_i = \tau_{pu} = L_{pu}/\omega_b * R_{pu}$$

the Inner current control, PI-3 and PI-4 based on the above Equations are

$$K_{PI-4} = K_{PI-3} = L_{pu} *f_{sw}/ \omega_b \quad (18)$$

$$T_{PI-4} = T_{PI-3} = L_{pu}/ \omega_b *R_{pu} \quad (19)$$

From the Equations (18) and (19) it is clear that tuning of the inner control parameters is dependent on Inductance and Resistance of AC system hence the AC system strength is considered in finding K_{PI-4} and T_{PI-4}.

4. Simulation and Results

4.1 System Description

The VSC-HVDC system of 300MW and ±180kV having Rectifier, AC system of 345kV at 60Hz and Inverter AC system of 230kV at 50Hz was modeled for different SCRs in RSCAD as shown in Figure 2. The circuit inside the blue box is simulated in small time step simulation and interfaced to the main circuit through small time step interface transformer.

4.2 Outer Control Parameters of the System

The VSC-HVDC model has DC voltage and AC voltage controls on both sides. The outer control parameters at

rectifier and inverter for DC voltage controls are obtained from Equations (16) and (17) and for AC voltage control are tuned from response of the system and are given in Table 2.

Table 2. Outer Control Parameters

Rectifier & Inverter	KPI-1	TPI-1	KPI-2	TPI-2
	18.7	0.003571	10	0.001

4.3 Inner Control Parameters of the System

The control parameters for rectifier are tuned for an SCR of 4.0 and kept constant throughout the simulation. The tuning of inner PI-controllers for the different system strengths from SCR 1.5 to SCR 4.0 was carried out for inverter using Equations (18) and (19). Table 3 gives control parameters considering the ac system strength while tuning. The L_{pu} in Equations (18) and (19) is sum of L_{SR}, L_{TR} and L_{FR} whereas R_{pu} is sum of R_{SR} and R_{TR}. As the X/R ratio is kept constant through out the simulation, time constant of the PI controllers is constant for rectifier and inverter. As the SCR at rectifier is maintained constant the controller gain is constant for rectifier.

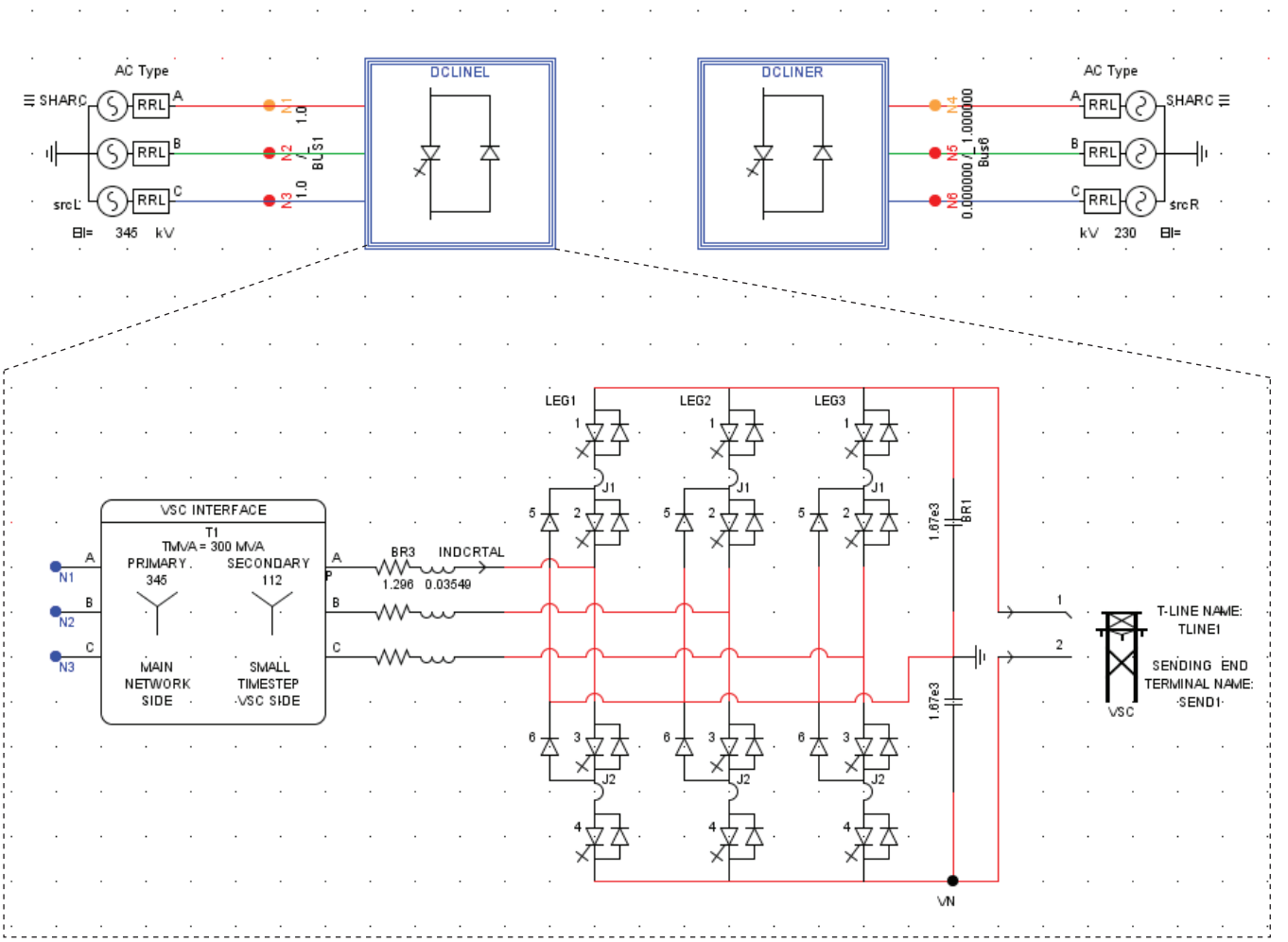

Figure 2. RSCAD model of the VSC-HVDC system and rectifier side circuit of VSC-HVDC.

4.4 Results and Discussion

The dynamic performance of VSC-HVDC when connected to the weak ac system with lower SCRs is difficult to achieve when compared to strong system with higher SCRs. Designed control parameters are evaluated for dynamic performance of the VSC-HVDC system for different CASEs listed in Table 3 and presented below.

CASE 1: Performance of VSC-HVDC link when connected to strong AC system

(a) Steady state

CASE 1 is with rectifier SCR of 4.0 and inverter SCR of 4.0. The system is strong on both sides. The steady state plots of VSC-HVDC link are shown in Figure 3 giving the parameters at the inverter end and Figure 4 giving the parameters at rectifier end for a strong AC system. The steady state values AC voltage, DC voltage and DC power at rectifier and inverter end are observed to be as per the rated values of the system.

(b) Three phase to ground fault at the inverter

For CASE 1, the three phase to ground fault is applied at 0.4 seconds for a fault duration of 100 milli seconds. It is observed that system is stable. Figure 5 and 6 give the parameters at inverter and rectifier end of VSC-HVDC link. From Figure 5 it is observed that the fault is at inverter side and the system is taking 300 msec to recover to the steady state powerflow after the fault. As the fault is at inverter side there is no dip in rectifier side voltages in Figure 6.

Table 3. Inner Control Parameters

CASE	SCR		KPI-3 & KPI-4		Ti3 & Ti4 (mS)	
	Rectifier	Inverter	Rectifier	Inverter	Rectifier	Inverter
1	4.0	4.0	2.607	3.128	0.015	0.018
2	4.0	3.5	2.607	3.417	0.015	0.018
3	4.0	3.0	2.607	3.794	0.015	0.018
4	4.0	2.5	2.607	4.332	0.015	0.018
5	4.0	2.0	2.607	5.134	0.015	0.018
6	4.0	1.5	2.607	6.473	0.015	0.018

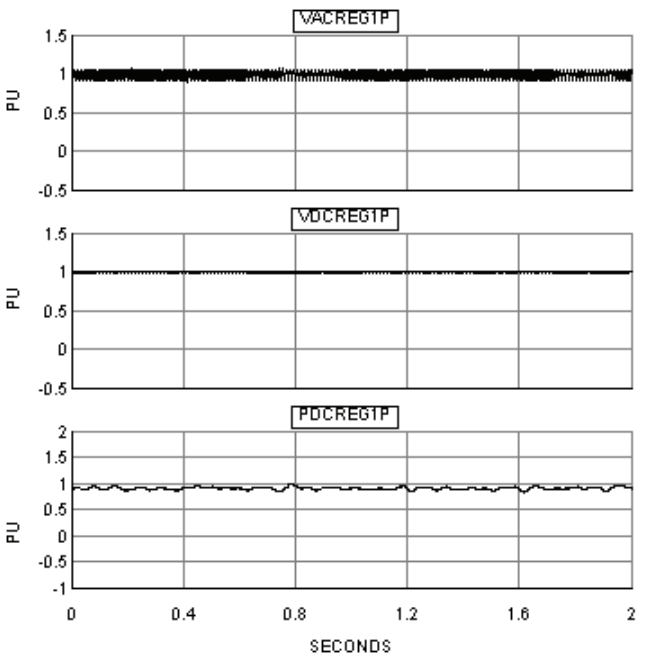

Figure 3. Case 1(a) – Inverter end (i) AC voltage (ii) DC voltage (iii) DC power.

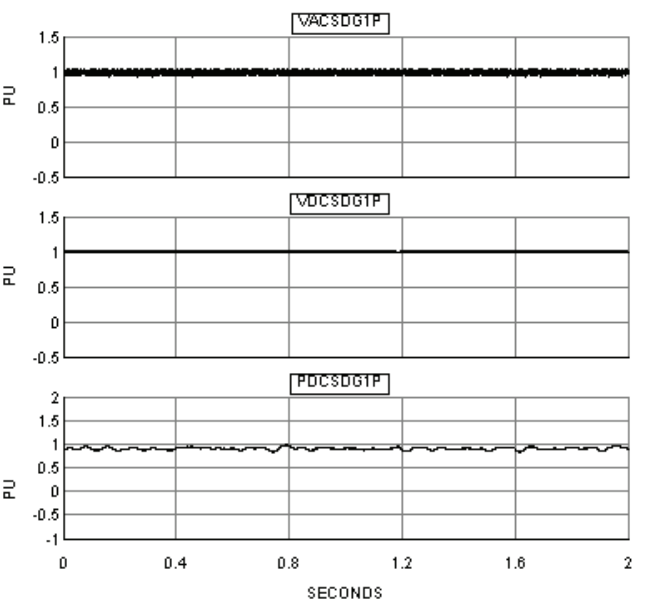

Figure 4. Case 1(a) – Rectifier end (i) AC voltage (ii) DC voltage (iii) DC power.

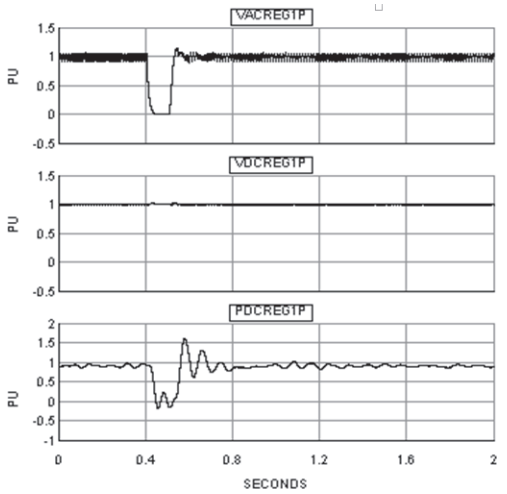

Figure 5. Case 1(b) – Inverter end (i) AC voltage (ii) DC voltage (iii) DC power.

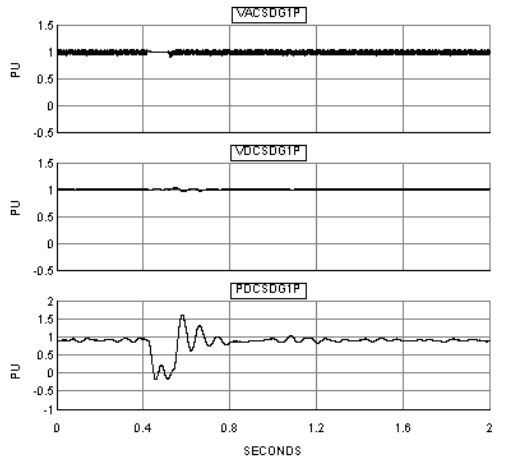

Figure 6. Case 1(b) – Rectifier end (i) AC voltage (ii) DC voltage (iii) DC power.

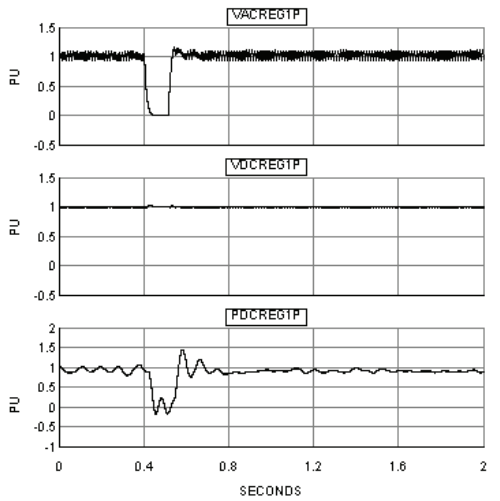

Figure 7. Case 5 – Inverter end (i) AC voltage (ii) DC voltage (iii) DC power.

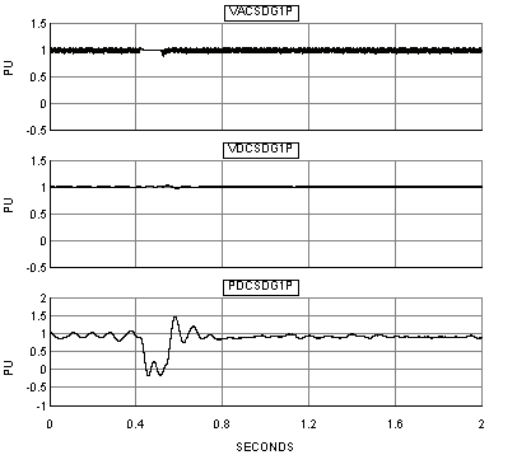

Figure 8. Case 5 – Rectifier end (i) AC voltage (ii) DC voltage (iii) DC power.

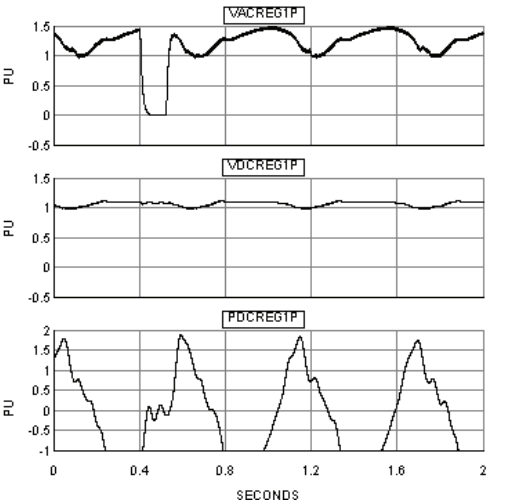

Figure 9. Case 6 – Inverter end (i) AC voltage (ii) DC voltage (iii) DC power.

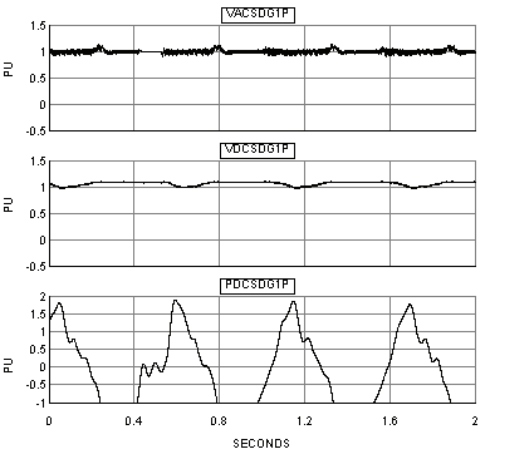

Figure 10. Case 6 – Rectifer End (i) AC voltage (ii) DC voltage (iii) DC power.

CASE 2 to 4: It is observed that system performance is stable so the results are not presented. However the results for CASE 5 and 6 for weak system are presented in next sections.

CASE 5: Performance of VSC-HVDC link when connected to weak AC system

Three phase to ground fault at the inverter

CASE 5 is with rectifier SCR of 4.0 and inverter SCR of 2.0. The system is strong on rectifier side and weak on inverter side. For CASE 5 also, the three phase to ground fault is applied in similar way of CASE 1 at 0.4 seconds for a fault duration of 100 milli seconds at the inverter side. It is observed that system is stable.

Figure 7 and 8 give the parameters at inverter and rectifier end of VSC-HVDC link. From Figure 7 it is observed that the fault is at inverter side and the system is taking 300 msec to recover to the steady state powerflow after the fault similar to CASE1. And the voltage dip is not observed in rectifier side in Figure 8. The method of tuning worked for the SCR of 2.0 at inverter side.

CASE 6: Performance of VSC-HVDC link when connected to weak AC system

CASE 6 is with rectifier SCR of 4.0 and inverter SCR of 1.5. The system is strong on rectifier side and weak on inverter side with SCR of 1.5. For CASE 6 it is observed that system is unstable even in steady state. Figure 9 and 10 give the parameters at inverter and rectifier end of VSC-HVDC link. From Figure 9 and 10 it is observed that the power flow through the DC line is not constant and system is unstable. The tuning method is working for a weak system of SCR up to 2.0 but not for SCR of 1.5

5. Conclusion

The control system for the VSC-HVDC link enables independent control of the active and reactive powers of the system. This feature is further elaborated in terms of the tuning controllers for various AC system strengths. Here, the control parameters of the PI regulators, namely, the proportional constant and integral constants are tuned using Modulus and Symmetrical Optimum techniques including the AC system impedance.

The simulation of the VSC-HVDC link is carried out in RSCAD simulation tool for varying system strengths at inverter side. It is found that the tuning technique followed is giving good results under steady-state and transient conditions from strong to weak system with SCR of 2.0. However for SCR of 1.5 this tuning method requires additional methods like reactive power support at the point of common coupling and tuning of PLL gains which will be addressed in future scope of work.

6. References

1. Flourentzou N, Agelidis VG, Demetriades GD. VSC-based HVDC power transmission systems: An overview. IEEE Transactions on Power Electronics. 2009; 24:592–602. https://doi.org/10.1109/TPEL.2008.2008441
2. IEEE guide for planning DC links terminating at AC locations having low short-circuit capacities; 1997. p. 1–216.
3. Jasim O, Dang HQS. Advanced control method for VSC-HVDC systems connected to weak grids. 18th European Conference on Power Electronics and Applications; 2016. https://doi.org/10.1109/EPE.2016.7695520
4. Fu X, Dessaint L.-A, Gagnon R, Zhou K, Cheng M. A comparative study of control schemes for VSCHVDC transmission system. 38th Annual Conference on IEEE Industrial Electronics Society, IECON; 2012.
5. Zhao C, Guo C. Complete-independent control strategy of active and reactive power for VSC based HVDC system. IEEE Power and Energy Society General Meeting; 2009. https://doi.org/10.1109/PES.2009.5275743
6. Schauder C, Mehta H. Vector analysis and control of advanced static VAR compensators. IEE Proceedings C Generation, Transmission and Distribution. 1993; 140:299. https://doi.org/10.1049/ip-c.1993.0044
7. Sakamoto IK, Sugimoto S, Sato T, Abe H. Development of a control system for a high-performance self-commutated AC/DC Converter. IEEE Transactions on Power Delivery. 1998; 13. https://doi.org/10.1109/61.660882
8. Nakajima T, Irokawa S. A control system for HVDC transmission by voltage sourced converters. IEEE Power Engineering Society Summer Meeting; 1999. https://doi.org/10.1109/PESS.1999.787474
9. Padiyar KR, Prabhu N. Modelling, control design and analysis of VSC based HVDC transmission systems. International Conference on Power System Technology 2004. PowerCon; 2004. https://doi.org/10.1109/ICPST.2004.1460096
10. Zhang G, Xu Z, Wang G. A linear and decoupled control strategy for VSC- based HVDC system. IEEE/PES Transmission and Distribution Conference and Exposition. Developing New Perspectives; Atlanta, USA. 2001 Nov 2.
11. Zhang G, Xu Z. Steady-state model for VSC based HVDC and its controller design. IEEE Conference Proceedings, Power Engineering Society Winter Meeting; 2001.

12. Chen H. Research on the control strategy of VSC based HVDC system supplying passive network. IEEE Power and Energy Society General Meeting; 2009 Jul 26-30. https://doi.org/10.1109/PES.2009.5275968
13. Ruihua S, Chao Z, Ruomei L, Xiaoxin Z. VSCs based HVDC and its control strategy. IEEE/PES Transmission and Distribution Conference; Asia and Pacific. 2005 Aug 18.
14. Du C, Sannino A, Bollen MHJ. Analysis of the control algorithms of voltage-source converter HVDC. IEEE Russia Power Tech. 2005 Jun 27-30.
15. Stan AI, Stroe D-I, Silva R. Control strategies for VSC-based HVDC transmission system. IEEE International Symposium on Industrial Electronics; 2011 Jun 27-30. https://doi.org/10.1109/ISIE.2011.5984362
16. Zhao C, Sun Y. Study on control strategies to improve the stability of multi-infeed HVDC systems applying VSC-HVDC. Canadian Conference on Electrical and Computer Engineering; 2006 May 7-10. https://doi.org/10.1109/CCECE.2006.277629
17. Du C, Bollen MHJ, Agneholm E, Sannino A. A new control strategy of a VSC–HVDC system for high-quality supply of industrial plants. IEEE Transactions on Power Delivery. 2007 Oct; 22:2386–94. https://doi.org/10.1109/TPWRD.2007.899622
18. Guo C, Zhang Y, Gole AM, Zhao C. Analysis of dual-infeed HVDC with LCC–HVDC and VSC–HVDC. IEEE Transactions on Power Delivery. 2012; 27:1529–37. https://doi.org/10.1109/TPWRD.2012.2189139
19. Liu Y, Chen Z. Power control method on VSC-HVDC in a hybrid multi-infeed HVDC system. IEEE Power and Energy Society General Meeting. 2012 Jul 22-26.
20. Guo C, Zhao C. Supply of an entirely passive AC network through a double-infeed HVDC system. IEEE Transactions on Power Electronics. 2010 Nov; 25:2835–41. https://doi.org/10.1109/TPEL.2010.2050214
21. Shilpa G, Manohar P. Hybrid HVDC system for multi-infeed applications. International Conference on Emerging Trends in Communication, Control, Signal Processing and Computing Applications (C2SPCA); 2013 Oct 10-11. https://doi.org/10.1109/C2SPCA.2013.6749393
22. Manohar P, Kelamane V, Kaushik D, Ahmed W. Improved controls for LCC-VSC hybrid HVDC system. International Conference on Circuits, Controls and Communications (CCUBE); 2013 Dec 27-28. https://doi.org/10.1109/CCUBE.2013.6718566
23. Bajracharya C, Molinas M, Suul J, Undeland TM. Understanding of tuning techniques of converter controllers for VSC-HVDC. Nordic Workshop on Power and Industrial Electronics; 2008 Jun 9-11.
24. Wang V, Beddard A, Barnes M, Marjanovic O. Analysis of active power control for VSC-HVDC. IEEE Transactions on Power Delivery. 2014 Aug; 29:1978–88. https://doi.org/10.1109/TPWRD.2014.2322498
25. Zhou JZ, Gole AM. VSC transmission limitations imposed by AC system strength and AC impedance characteristics. 10th IET International Conference on AC and DC Power Transmission (ACDC 2012); 2012 4-5 Dec.
26. Zhou JZ, Ding H, Fan S, Zhang Y, Gole AM. Impact of short-circuit ratio and phase-locked-loop parameters on the small-signal behavior of a VSC-HVDC Converter. IEEE Transactions on Power Delivery. 2014 Oct; 29:2287–96. https://doi.org/10.1109/TPWRD.2014.2330518
27. Wu G, Liang J, Zhou X, Li Y, Egea-Alvarez A, Li G, Peng H, Zhang X. Analysis and design of vector control for VSC-HVDC connected to weak grids. CSEE Journal of Power and Energy Systems. 2017 Jun; 3:115–24. https://doi.org/10.17775/CSEEJPES.2017.0015
28. Lu S, Xu Z, Xiao L, Jiang W, Bie X. Evaluation and enhancement of control strategies for vsc stations under weak grid strengths. IEEE Transactions on Power Systems. 2018 Mar; 33:1836–47. https://doi.org/10.1109/TPWRS.2017.2713703
29. Arani MFM, Mohamed YA-RI. Analysis and performance enhancement new line of vector-controlled VSC in HVDC links connected to very weak grids. IEEE Transactions on Power Systems. 2017 Jan; 32:684–93. https://doi.org/10.1109/TPWRS.2016.2540959
30. Suul JA, D'Arco S, Rodriguez P, Molinas M. Impedance-compensated grid synchronisation for extending the stability range of weak grids with voltage source converters. IET Generation, Transmission and Distribution. 2016 Apr; 10:1315–26. https://doi.org/10.1049/iet-gtd.2015.0879
31. Safdarian F, Ardehali MM, Gharehpetian GB, Performance of optimal controller of VSC-HVDC systems in weak networks. IAJC-ISAM International Conference; 2014. PMCid:PMC4126250
32. Muriuki J, Muriithi C, Ngoo L, Nyakoe G. Wider range of tuning the proposed VSC-HVDC system for improved controller performance. International Journal of Electrical Engineering and Technology (IJEET). 2016; 7(6):100–16.
33. Li Y, Yang S, Wang K, Zeng D."Research on PI controller tuning for VSC-HVDC system. International Conference on Advanced Power System Automation and Protection; 2011 Oct 16-20. https://doi.org/10.1109/APAP.2011.6180414
34. Li G, Yin M, Zhou M, Zhao C. Modeling of VSC-HVDC and control strategies for supplying both active and passive systems. IEEE Power Engineering Society General Meeting; 2006 Jun 18-22.
35. Geetha RS, Deekshit R, Lal G. Controllers for A VSC-HVDC link connected to a weak AC system. IOSR Journal of Electrical and Electronics Engineering. 2015 Jan-Feb; 10(1):18–32.